microbial biotechnology

Open Access

Activity of bacteria isolated from bats against *Pseudogymnoascus destructans* in China

Zhongle Li,[1,2] Aoqiang Li,[2,3] Joseph R. Hoyt,[4] Wentao Dai,[2] Haixia Leng,[2] Yanfei Li,[5] Wei Li,[5] Sen Liu,[6] Longru Jin,[2] Keping Sun[2,3] and Jiang Feng[1,2]

[1]*College of Animal Science and Technology, Jilin Agricultural University, Changchun, 130018, China.*
[2]*Jilin Provincial Key Laboratory of Animal Resource Conservation and Utilization, Northeast Normal University, 2555 Jingyue Street, Changchun, 130117, China.*
[3]*Key Laboratory of Vegetation Ecology, Ministry of Education, Changchun, 130024, China.*
[4]*Department of Biological Sciences, Virginia Polytechnic Institute, Blacksburg, VA 24060, USA.*
[5]*College of Chinese Medicine Materials, Jilin Agricultural University, Changchun, 130118, China.*
[6]*Institute of Resources and Environment, Henan Polytechnic University, Jiaozuo, 454000, China.*

Summary

White-nose syndrome, a disease that is caused by the psychrophilic fungus *Pseudogymnoascus destructans*, has threatened several North America bat species with extinction. Recent studies have shown that East Asian bats are infected with *P. destructans* but show greatly reduced infections. While several factors have been found to contribute to these reduced infections, the role of specific microbes in limiting *P. destructans* growth remains unexplored. We isolated three bacterial strains with the ability to inhibit *P. destructans*, namely, *Pseudomonas yamanorum* GZD14026, *Pseudomonas brenneri* XRD11711 and *Pseudomonas fragi* GZD14479, from bats in China. *Pseudomonas yamanorum*, with the highest inhibition score, was selected to extract antifungal active substance. Combining mass spectrometry (MS) and nuclear magnetic resonance (NMR) spectroscopy analyses, we identified the active compound inhibiting *P. destructans* as phenazine-1-carboxylic acid (PCA), and the minimal inhibitory concentration (MIC) was 50.12 μg ml^{-1}. Whole genome sequencing also revealed the existence of PCA biosynthesis gene clusters. Gas chromatography-mass spectrometry (GC-MS) analysis identified volatile organic compounds. The results indicated that 10 ppm octanoic acid, 100 ppm 3-tert-butyl-4-hydroxyanisole (isoprenol) and 100 ppm 3-methyl-3-buten-1-ol (BHA) inhibited the growth of *P. destructans*. These results support that bacteria may play a role in limiting the growth of *P. destructans* on bats.

Received 2 November, 2020; accepted 20 January, 2021.
For correspondence. *E-mail sunkp129@nenu.edu.cn; Tel. (+86) 431 8916 5610; Fax (+86) 431 84533101. **E-mail fengj@nenu.edu.cn; Tel. (+86) 431 84533101; Fax (+86) 431 84533101.
Microbial Biotechnology (2022) **15**(2), 469–481
doi:10.1111/1751-7915.13765
Funding information
This work was supported by the National Natural Science Foundation of China (grant numbers 31961123001, 31770403, 31570390 and 31670390), Jilin Provincial Natural Science Foundation (grant number 20180101272JC), and the Program for Introducing Talents to Universities (B16011) and the US National Science Foundation (DEB-1911853).

Introduction

Over the past several decades, fungal diseases have caused widespread declines in wildlife populations, including amphibians affected by chytridiomycosis, snakes impacted by snake fungal disease and bats affected by white-nose syndrome (WNS) (Skerratt *et al.*, 2007; Langwig *et al.*, 2012; Lorch *et al.*, 2016; Scheele *et al.*, 2019). The application of probiotics to treat fungal pathogens has achieved varying degrees of success in the fields of human and veterinary medicine, agriculture and aquaculture (Tan *et al.*, 2016; Kerry *et al.*, 2018; Markowiak *et al.*, 2019; Xia *et al.*, 2020). While beneficial bacteria are used less frequently to combat wildlife disease, there is evidence that naturally occurring microbes may contribute to differences in infection severity.

White-nose syndrome, an emerging infectious disease of hibernating bats in North America, is caused by the psychrophilic fungus, *Pseudogymnoascus destructans* (Gargas *et al.*, 2009; Lorch *et al.*, 2011; Warnecke *et al.*, 2012). WNS has killed millions of bats in North America from 2006, with several species being severely affected (Frick *et al.*, 2010; Langwig *et al.*, 2012). Bacteria and fungi isolated from bats and the environment have been shown to inhibit the growth of *P. destructans in vitro* (Hoyt *et al.*, 2015; Raudabaugh and Miller, 2015; Micalizzi *et al.*, 2017; Rusman *et al.*, 2020), and application of *Pseudomonas fluorescens* on bat skin over winter was recently shown to increase survival for one species of

bat (Hoyt *et al*., 2019). *P. destructans* conidia have also been shown to be inhibited by the volatile organic compounds produced by *R. rhodochrous* (Cornelison *et al*., 2014) and trans-farnesol, a sesquiterpene made by the yeast *Candida* (Raudabaugh and Miller, 2015). In addition, *Oidiodendron truncatum* was shown to produce various compounds that reduced the growth of *P. destructans* at low concentrations (Rusman *et al*., 2020). These studies demonstrated that bacteria were likely to contribute to differences in infections among individuals and species in bats.

Hibernating bats across Europe and Asia have been shown to be infected with *P. destructans,* but the symptoms of this disease are greatly reduced, and fungal load and prevalence are lower than bats that suffer mortality in North America (Wibbelt *et al*., 2010; Hoyt *et al*., 2016a,b). While the timing of transmission has been found to be an important factor for bats surviving with this disease across Eurasia there is likely a multitude of factors that contribute to bats persistence with this disease (Hoyt *et al*., 2020). We hypothesized that skin microbiota may also contribute to the reduction of infection by *P. destructans*.

In this study, we collected cutaneous bacteria from two bats species, *Rhinolophus ferrumequinum* and *Myotis petax*, in late hibernation from north-east and central China. We isolated and identified bacteria that inhibited the growth of *P. destructans* using *in vitro* challenge assays and analysed the antifungal metabolites produced by the bacteria isolate with the highest inhibitory effect. In addition, we examined the volatile organic compounds produced by this same isolate with the highest inhibition rate. Finally, we also examined the existence of gene clusters associated with these active substances. Our results provide evidence for a potential mechanism of disease resistance for *P. destructans* in East Asian bats by their skin microbes.

Results

Isolation, screening and identification of bacteria with anti-P. destructans activity

We isolated 90 total bacterial morphologies from the 25 samples collected from *R. ferrumequinum* (15) and *M. petax* (10). Agar plate challenge assays results showed that three bacterial isolates had the ability to inhibit the growth of *P. destructans*. One isolate, GZD14026, was from two individuals of *M. petax* in Ge-zi Cave. Two isolates, GZD 14479 and XRD11711, were from one individual of *R. ferrumequinum* in Ge-zi Cave and two individuals of *R. ferrumequinum* in Temple Cave, respectively (Table 1). An obvious inhibition zone appeared around isolate GZD14026. Concurrently, different inhibition modes were presented in the isolate GZD14479, while a small inhibition halo was observed surrounding isolate XRD14479 (Fig. 1A). These results suggest that bacterial isolate GZD14026 had the strongest inhibitory effect on *P. destructans*.

We further evaluated the inhibition rate of the above three bacterial isolates in cell-free supernatant assay. The results displayed that isolate GZD14026 had the strongest inhibition effect, with an average inhibition score of 71.33%, while isolate GZD14479 and XRD11711 were 33.27% and 22.90%, respectively. The inhibition score of isolate GZD14026 was more than double those of isolate GZD14479 and XRD11711 (Tukey's tests: isolate GZD14026–isolate GZD14479, $P < 0.001$; isolate GZD14026–isolate XRD11711, $P < 0.001$; Fig. 1B), so we focused on the chemical mechanism underlying the strong inhibition produced by isolate GZD14026.

The 16S rRNA genes and three housekeeping genes *gyrB*, *rpoD* and *rpoB* were concatenated for a multilocus sequence analysis (MLSA) of these three bacterial strains, which were sequenced and compared with other strains in the GenBank database. The results revealed that the concatenated sequences of these three bacterial strains were all from the genus *Pseudomonas*, with greater than 99% gene sequence similarities with three different *Pseudomonas* spp., *Pseudomonas yamanorum*, *Pseudomonas fragi* and *Pseudomonas brenneri*. Therefore, the three bacterial strains were subsequently referred to as *P. yamanorum* GZD14026, *P. fragi* GZD 14479 and *P. brenneri* XRD11711, respectively (Table 1).

Morphological changes of P. destructans mycelium

Scanning electron microscopy (SEM) showed alterations of *P. destructans* mycelium when exposed to *P. yamanorum* GZD14026 cell-free supernatant after 14 days. The surfaces of the mycelium in the non-exposed group were

Table 1. Bacteria isolated from *R. ferrumequinum* and *M. petax* used in agar plate challenge assays.

Label	Bat species	Collection Province	Bat numbers	Collection date (late hibernation)	Bacterial taxonomy
GZD14026	*M. petax*	Ge-zi Cave, Jilin	2	9-Apr-18	*Pseudomonas yamanorum*
GZD14479	*R. ferrumequinum*	Ge-zi Cave, Jilin	1	9-Apr-18	*Pseudomonas fragi*
XRD11711	*R. ferrumequinum*	Temple Cave, Liaoning	2	6-Apr-18	*Pseudomonas brenneri*

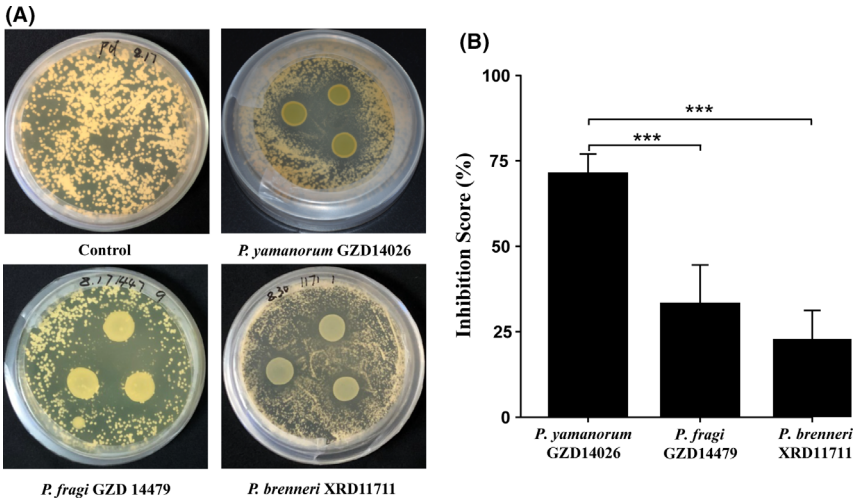

Fig. 1. Anti- *P. destructans* activity in challenge assays with cutaneous bacteria. A. Bacteria were inoculated onto plates previously inoculated with *P. destructans* and then incubated during 14 days (13°C). Control (only *P. destructans*). B. Comparison of the inhibition score of *P. destructans* from three bacterial strains. Data represent the mean ± standard deviation from twelve independent experiments. *** represents $P < 0.001$.

smooth, slender, uniform thickness, plump and round (Fig. 2A–C). In contrast, the mycelium morphology of the group exposed to GZD14026 became malformed, short with uneven thickness, and many branches were fractured (Fig. 2D–F).

Isolation, purification and identification of active compounds with anti-P. destructans activity

To obtain the active compounds that inhibited the growth of *P. destructans* from *P. yamanorum* GZD 14026, 8.3 g of crude extract was acquired from 30 l of LB liquid fermentation by extraction with dichloromethane. This was mixed with an equal weight of silica gel and then eluted. An anti-*P. destructans* compound was detected in a single band with an *Rf* of 0.78 by thin-layer chromatography (TLC) analysis, indicating the existence of a single compound. This antifungal compound was further detected by semi-preparative high-performance liquid chromatography (HPLC) and appeared as a single peak at 12.11 min (Fig. 3A), which was a lemon-yellow crystalline powder with inhibition rate against *P. destructans* of 60.23%.

We used the ultraviolet-visible spectra (UV/Vis), mass spectrometry (MS) and nuclear magnetic resonance (NMR) spectroscopy to identify the active compound structure from *P. yamanorum* GZD 14026. Strong absorption peaks were observed at 206.7 nm, 251.4 nm and 364.1 nm using UV/Vis spectra analysis (Fig. S1A). MS results revealed two strong molecular ion peaks at *m/z* 225.21 $[M + H]^+$ and *m/z* 207.21 $[M - OH]^+$ (Fig. 3B). The results of ^1H NMR and ^{13}C NMR spectra were described in (Fig. S1B and Table 2).

All of the spectral detection results showed that the anti-*P. destructans* active compound of *P. yamanorum* GZD 14026 was phenazine-1-carboxylic acid (PCA), with the molecular formula $C_{13}H_8N_2O_2$ (Fig. 3C and Fig. S1C), which was consistent with the conclusions proposed by Lee *et al*., 2003. The minimal inhibitory concentration (MIC) of PCA against *P. destructans in vitro* was 50.12 μg ml^{-1}, and the half maximal inhibitory concentration (IC_{50}) was 32.08 μg ml^{-1}.

Whole genome comparison involved in PCA biosynthesis

The whole genome of *P. yamanorum* GZD 14026 was 6 947 460 bp in length, with a GC content of 59.04%. A total of 6886 genes were identified from this genome, including 6797 genes encoding proteins. Additionally, genome analysis suggested that *P. yamanomum* GZD 14026 produced secondary metabolites of phenazine. We next investigated the genes involved in PCA biosynthesis from *P. yamanomorum* GZD 14026, and we compared them with common PCA-producing bacterial strains, including *P. chlororaphis* GP72 (Shen, *et al*., 2012) and *P. fluorescens* 2-79 (Mavrodi, *et al*., 1998). The results revealed that, compared with the genes of the PCA biosynthetic operon from *P. chlororaphis* GP72, *phzA* to *phzG* had 88.73–94.36% and 87.80–93.03% homology with *P. fluorescens* 2-79 (Table 3). Therefore, this suggested that *P. yamanorum* GZD 14026 could produce PCA.

Evaluation, identification and verification of volatile organic compounds with anti-P. destructans activity

Pseudomonas yamanorum GZD 14026 was co-cultured with *P. destructans*, and after 14 days, we found that the

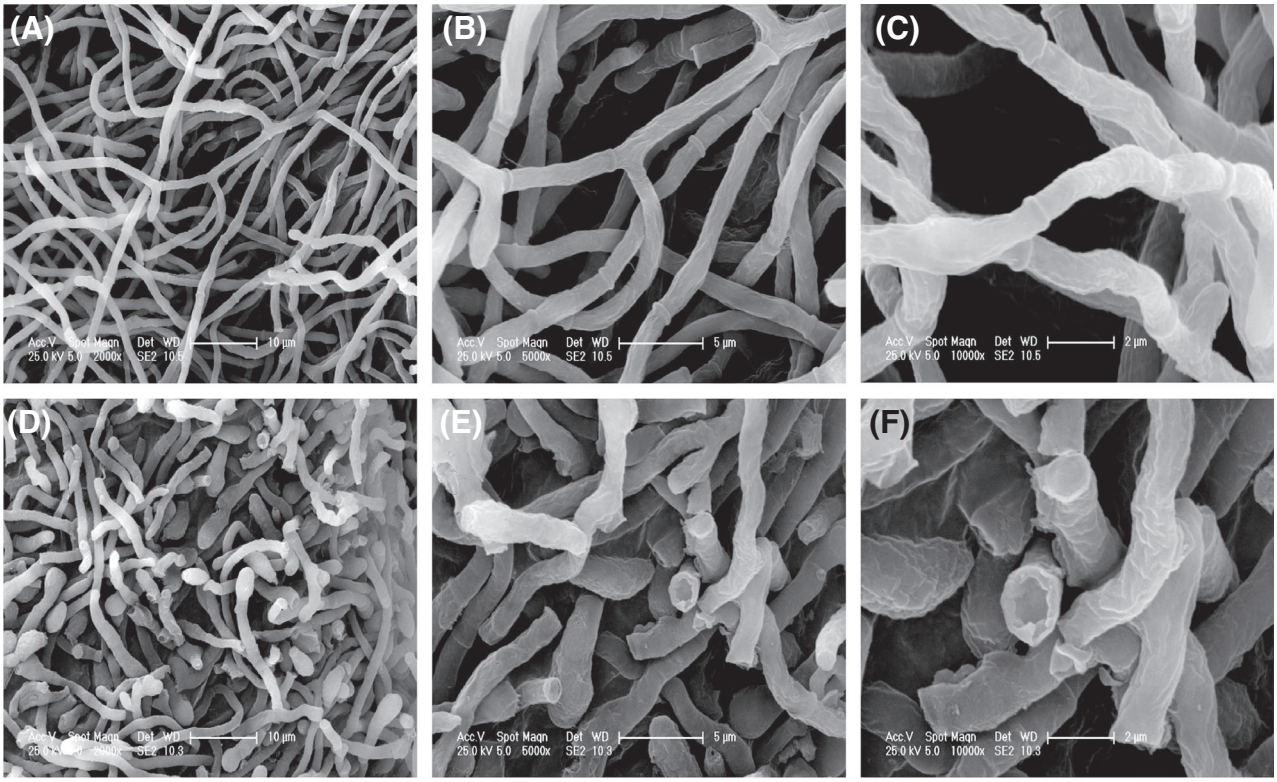

Fig. 2. SEM observation of mycelial changes of *P. destructans* by treatment with *P. yamanorum* GZD 14026. A–C. Control (without *P. yamanorum* GZD 14026), *P. destructans* mycelium grows normally over 14 days (13°C). D–F. Inoculation with *P. yamanorum* GZD 14026 after 14 days (13°C), and the growth of *P. destructans* was inhibited by changing the mycelium. Magnification 2000 × (A, D: bar 10 μm), 5000 × (B, E: bar 5 μm) and 10 000 × (C, F: bar 2 μm).

number of *P. destructans* conidia was dramatically reduced and malformed when compared with control samples, suggesting that volatile organic compounds (VOCs) were also being released from *P. yamanorum* GZD 14026 and were impacting the growth of *P. destructans* (Fig. 4A).

We used gas chromatography-mass spectrometry (GC-MS) to identify the volatile organic compounds produced by *P. yamanorum* GZD 14026, and a total of 16 compounds were detected after removing controls (Table S1), of which three compounds were demonstrated to inhibit the growth of *P. destructans*, namely, octanoic acid, 3-methyl-3-butene-1-alcohol (isoprenol) and 3-tert-butyl-4-hydroxyanisole (BHA). Among the best inhibitory effect was octanoic acid, which generated a large inhibition circle at 10 ppm. BHA had similar results at 100 ppm, while almost no fungal growth was seen with 100 ppm isoprenol (Fig. 4B).

Discussion

In this study, we isolated three bacterial strains with the ability to inhibit the growth of *P. destructans* from *R. ferrumequinum* and *M. petax* from two localities (Table 1). This was similar to the number of active strains ($n = 6$) isolated in Hoyt and colleagues (2015), but less than others, such as ($n = 28$) from Micalizzi *et al.* (2017) and ($n = 32$) from Hamm and colleagues (2017). This numerical difference might be due to the method of our inhibition assays (McArthur *et al.*, 2017). In this study, we used the same method to screen for anti-*P. destructans* bacteria as Hoyt and colleagues (2015), but this was different from others (Micalizzi *et al.*, 2017; Hamm *et al.*, 2017). In addition, the number of bats ($n = 25$) we collected was also less than those ($n = 40$) from Hoyt and colleagues (2015) and ($n = 101$) Hamm and colleagues (2017), which might result in the relatively low number of active strains isolated in this study. Actually, it is a real possibility that the growth of *P. destructans* is inhibited by the interactions of multiple microorganisms. In future work, we intend to optimize the method of inhibition experiments and expand sample sizes to screen more probiotic strains.

Coincidentally, the three bacterial isolates identified in this work were from the genus *Pseudomonas*. It is well-known that *Pseudomonas* is widely distributed in the environment and has been also found on mammals, amphibians, reptiles and plants (Gholami *et al.*, 2017; Brunetti *et al.*, 2019; Brockmann *et al.*, 2020; Fernandez

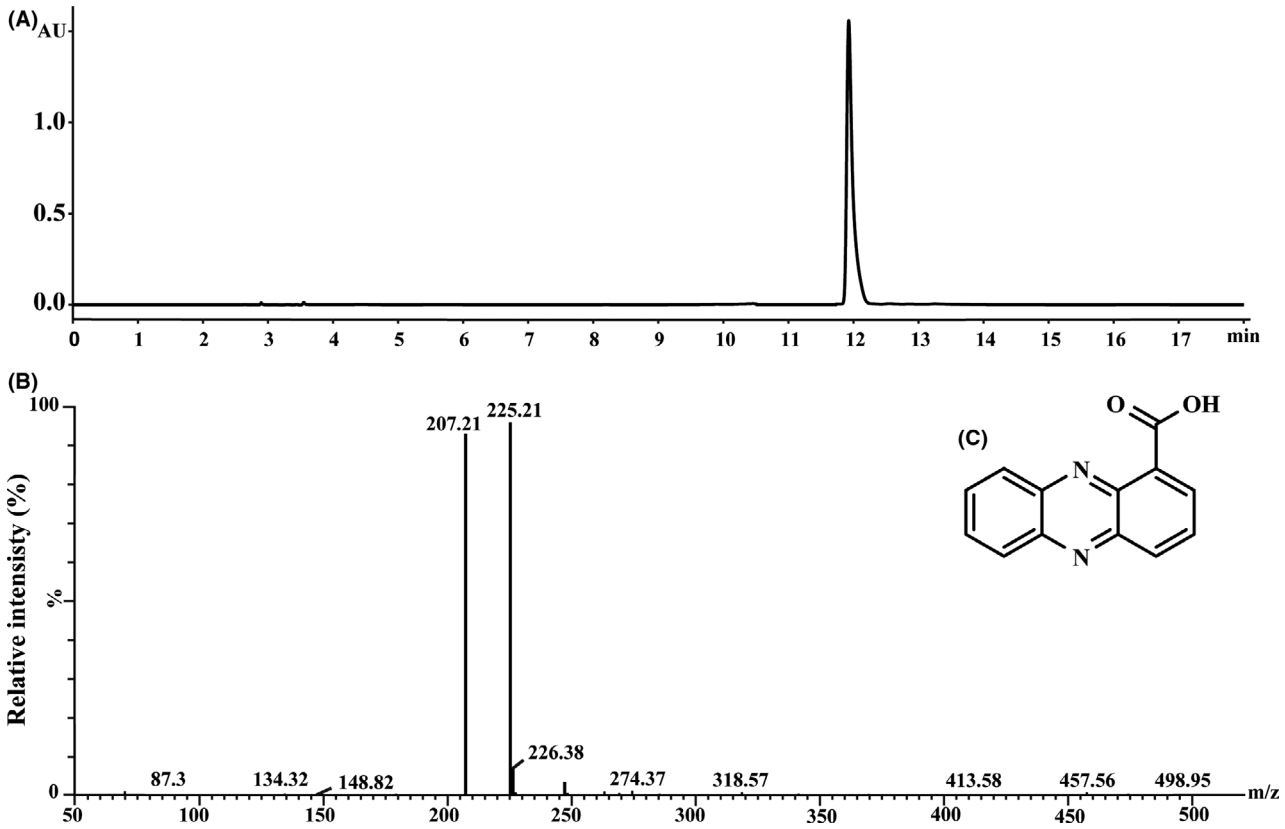

Fig. 3. Analysis of the active compounds against *P. destructans* from *P. yamanorum* GZD 14026. A. RP-HPLC (250 nm) identification of the active compound. Absorbance × Retention Time. B. MS detection of the active compound. C. The structure of the phenazine-1-carboxylic acid (PCA).

Table 2. ^{1}H and ^{1}C spectral data of active compounds from *P. yamanorum* GZD 14026 against *P. destructans*.

Carbon no.	^{13}C, δ^{a}	^{1}H δ^{b} (m^{c}, *J* in H_Z)
1	125.2	—
2	130.5	8.57 (dd, 7.0, 1.5)
3	137.7	8.31-8.39 (m)
4	135.4	9.01 (dd, 8.7, 1.5)
4a	140.1	—
5a	140.3	—
6	132.0	7.99-8.08 (m)
7	128.2	8.31-8.39 (m)
8	130.3	8.31-8.39 (m)
9	133.5	7.99-8.08 (m)
9a	143.6	—
10a	144.3	—
COOH	166.2	15.61(s)

a. 125 MHz, chemical shift in ppm.
b. 500 MHz, chemical shift in ppm.
c. Abbreviations of signal multiplicity are (s): singlet, (dd): doublet of doublets, (m): multiplet.

et al., 2020). *Pseudomonas* bacteria have been demonstrated to inhibit the growth of several relevant fungal diseases, including chytridiomycosis and white-nose syndrome in North America. *Pseudomonas* spp. from the skin bacterial communities of frogs have been shown to restrict *Batrachochytrium dendrobatidis* at an inhibition rate over 90% (Kruger, 2020), and Hoyt and colleagues (2015) demonstrated that most of the bacteria isolated from bats that could inhibit *P. destructans* growth came from the genus *Pseudomonas*.

Pseudomonas is well-known for its antibacterial activity and can produce a large number of secondary metabolites, such as phenazines, pyrrolnitrin, pyoluteorin, 2,4-diacetylphloroglucinol and peptides (Schnider *et al*., 1995; Bender *et al*., 1999; Nielsen *et al*., 2002; Lee *et al*., 2003; Isnansetyo *et al*., 2003). Antibiotic-producing *Pseudomonas* can be highly effective biocontrol agents (Wang *et al*., 2020; Kamou *et al*., 2020). In this study, an anti-*P. destructans* active substance was separated from the culture medium of *P. yamanorum* GZD 14026. Using UV/Vis, MS and NMR detection, we revealed that phenazine compounds, namely phenazine-1-carboxylic acid, of which 32.08 $\mu g\ ml^{-1}$ of PCA inhibited *P. destructans* with an efficiency of 50%, was responsible for this strong inhibitory activity. The whole genome of *P. yamanorum* GZD 14026 had PCA-producing gene clusters (Table 3).

Phenazine compounds can be extracted from various microorganisms and have been recognized as antibiotics

Table 3. Identification of the *phz* genes of *P. yamanorum* GZD 14026 with other *Pseudomonas* spp.

Gene	Accession number	Homology to *P. yamanorum* GZD 14026		Description
		P. chlororaphis GP72	*P. fluorescens* 2-79	
phzA	GZD14026_3940	92.07%	87.80%	Phenazine biosynthesis protein
phzB	GZD14026_3941	94.36%	93.03%	Phenazine biosynthesis protein
phzC	GZD14026_3942	90.72%	88.44%	3-Deoxy-7-phosphoheptulonate synthase
phzD	GZD14026_3943	93.69%	90.61%	Isochorismatase family protein
phzE	GZD14026_3944	91.38%	88.26%	Anthranilate synthase
phzF	GZD14026_3945	93.79%	89.73%	Phenazine biosynthesis protein isomerase
phzG	GZD14026_3946	88.73%	88.64%	Pyridoxamine-5′-phosphate oxidase

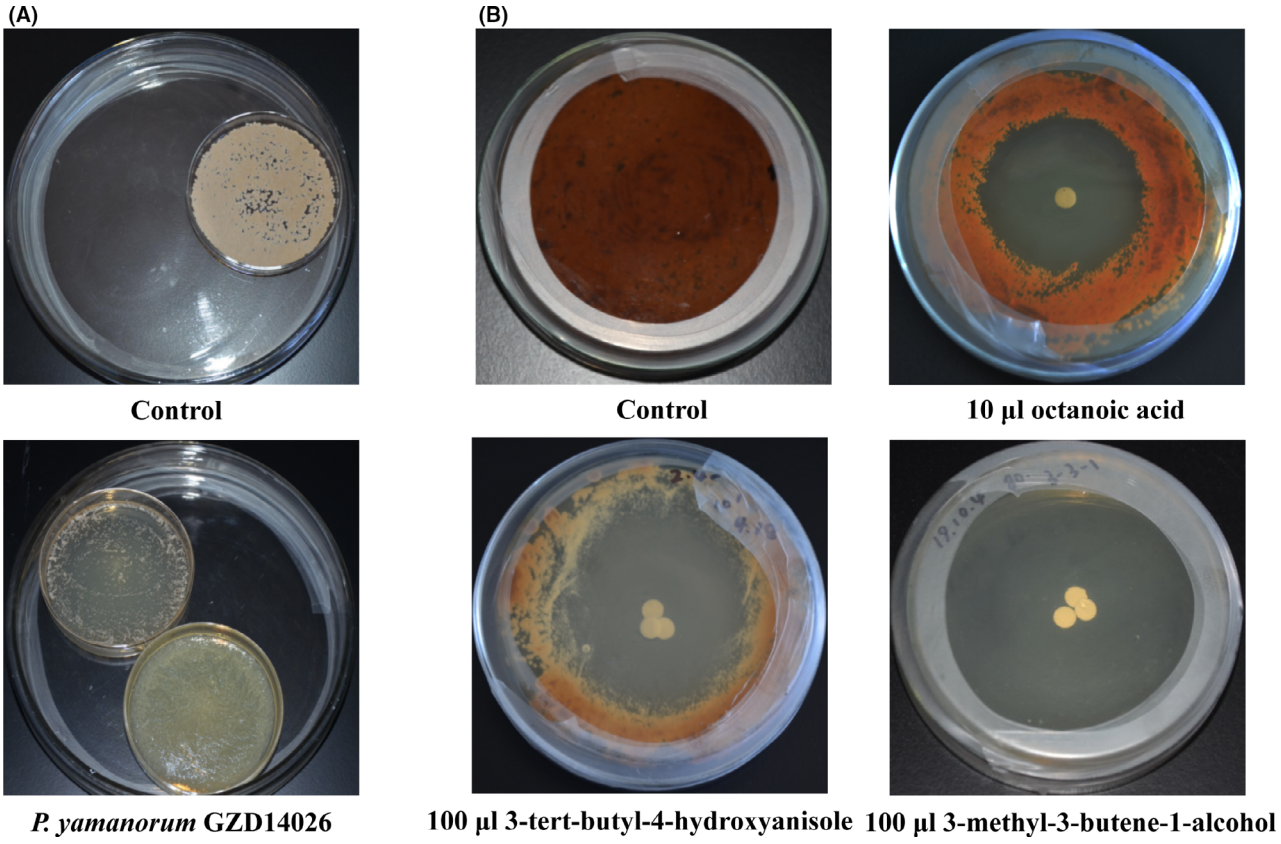

Fig. 4. Evaluation and verification of volatile organic compounds from *P. yamanorum* GZD 14026 working against *P. destructans*. A. Co-cultured *P. yamanorum* GZD 14026 with *P. destructans* after 14 days (13°C). Control (only *P. destructans*). B. Four volatile compounds inoculated with *P. destructans* after 14 days (13°C). Control (100 µl 95% ethanol and *P. destructans*). The image of the front side (A) and the back side (B) of the culture medium.

against plant diseases, as well as inducing systemic resistance in plants (Santos Kron *et al.*, 2020; Jin *et al.*, 2020). PCA is a very important compound widely present in microbial metabolites from *Pseudomonas*, *Streptomycetes* and *Bacillus* spp. (Kim, 2000; Xiong *et al.*, 2017). Additionally, PCA is used as a biocontrol agent against various plant pathogens in China (Zhou *et al.*, 2010). The inhibitory effect of PCA on fungi may be a complicated process, which involves multiple complex physiological processes such as cell wall structure and synthesis, cell membrane integrity, intracellular redox system, protein sorting and vesicle transport, and chromatin remodelling (Xu *et al.*, 2015; Zhu *et al.*, 2017). Moreover, PCA is an ideal compound for the development of microbial metabolites because of its stable chemical structure, low toxicity and compatibility with the environment (Yuan *et al.*, 2008), and represents a new type of microorganism-derived pesticide (Huasong *et al.*,

2020). Therefore, it could be used in conservation strategies combating white-nose syndrome in bats. The current studies on phenazines have primarily been in relation to the genus *Pseudomonas*, specifically *P. fluorescens*, *P. chlororaphis* and *P. aeruginosa*. *P. fluorescens* has been found to only synthesize PCA; however, *P. chlororaphis* and *P. aeruginosa* can also produce some other phenazine derivatives, such as phenazine-1-amide (PCN), pyocyanin (PYO), 1-hydroxyphenazine (1-OH-PhZ), 2-hydroxy-phenazine-1-carboxylic acid (2-OH-PCA), which all have demonstrated antimicrobial activity (Mavrodi *et al*., 2006; Mossine *et al*., 2018). However, some phenazine compounds also have anti-cancer, antimalarial and anti-parasitic biological activities, which has attracted increasing attention to these compounds (Haas, *et al*., 2000; Laursen and Nielsen, 2004; Rajkumar *et al*., 2020).

Challenge assays results showed that the *P. yamanorum* GZD 14026 isolated from the skin of *M. petax* during hibernation showed the strongest inhibitory effect, with an inhibition rate of 71.33%. SEM further demonstrated that *P. yamanorum* GZD 14026 caused *P. destructans* mycelium morphology to undergo significant changes, indicating that the growth of mycelium was seriously affected. The *P. destructans* mycelium was affected by direct contact with the yellow active substance (PCA) secreted by *P. yamanorum* GZD14026 in SDA. PCA played a role in changing the *P. destructans* mycelium morphology. Similarly, *Vibrio anguillarum* appeared to have deformed mycelia when this fungus was treated with PCA (Zhang *et al*., 2017). However, there may be other factors influencing mycelium morphology, such as volatile organic compounds (VOCs). *P. destructans* mycelium growth and conidiation germination were persistently suppressed by the VOCs produced by *R. rhodochrous* (Cornelison *et al*., 2014). Therefore, the effect of *P. yamanorum* GZD14026 on the inhibition of *P. destructans* mycelium was a multiple action process. Other studies have shown that *P. yamanomum* showed strong inhibitory effects on other fungal pathogens, including *Botrytis cinerea* (Vignatti *et al*., 2020), *Fusarium solani* (Bahroun *et al*., 2018) and other Gram-negative and Gram-positive bacteria (Arnau *et al*., 2015).

In this study, it was proposed for the first time that *P. yamanomum* GZD 14026 produced not only PCA but also a series of VOCs. Specifically, 10 ppm octanoic acid, 100 ppm BHA and 100 ppm isoprenol significantly inhibited the growth of *P. destructans*. Octanoic acid was also isolated from *Megasphaera* (Jeon *et al*., 2017). Studies have shown that octanoic acid and its derivatives can effectively kill aquaculture pathogens and a variety of food-borne pathogens, including *Escherichia coli* O157:17, *Enterobacter sakazakii* and *Listeria monocytogenes* (Annamalai *et al*., 2004; Nair *et al*., 2004; Kollanoor *et al*., 2007). The volatile compounds extracted from the vegetative phase of *Polygonum bistorta* were majorly isoprenol, and illustrated their abilities against *Paenibacillus larvae* and *Bacillus subtilis* (Cecotti *et al*., 2012). Isoprenol is also found in *Escherichia* and *Corynebacterium* (George *et al*., 2015; Sasaki *et al*., 2019). BHA is an antioxidant that can be added to foods, and also kills a wide range of pathogenic bacteria, such as *Salmonella typhimurium*, *Staphylococcus aureus*, *Vibrio parahaemolyticus* and *Aspergillus parasiticus* (Chang and Branen, 1975; Pierson *et al*., 1980). One study isolated BHA from *Chlorococcum* (Olasehinde *et al*., 2020). The mechanism of action of VOCs was to inhibit the growth of fungal mycelium, spore formation and germination (Elkahoui *et al*., 2015). At present, VOCs have been used in *P. destructans* hibernaculum sediment, and they have the characteristics of fast action and good killing effect (Micalizzi and Smith, 2020). These VOCs can be used as an effective management strategy to reduce the environmental exposure of bats to *P. destructans* in hibernacula.

Based on our results, the bacteria isolated from the bat skin can inhibit the growth of *P. destructans* under laboratory conditions, and secrete a variety of metabolites and volatile compounds. In future work, it is necessary to inoculate bats with either the probiotic *P. yamanorum* GZD 14026 or those active substances produced by this strain, such as PCA, octanoic acid, isoprenol or BHA, to test the inhibitory effect on *P. destructans* growth on living hibernating bats *in vivo*, which will have important significance for protecting bats from white-nose syndrome.

Experimental procedures

Pseudogymnoascus destructans

Pseudogymnoascus destructans JHCN111a (Hoyt *et al*., 2016b) was isolated from *M. petax* in north-eastern China during March 2015, and was cultured on Sabouraud dextrose agar (SDA) at 13 $\pm$ 1°C, which was within the optimum temperature range. *P. destructans* cultures were stored in Sabouraud dextrose broth (SDB) amended with 20% sterile glycerol at −80°C. To obtain conidiospores of *P. destructans*, cultures were incubated at 13 $\pm$ 1°C for 21 days on SDA. Fresh spore suspensions were obtained each time for subsequent experiments.

Bacterial isolation

We collected cutaneous bacteria samples in late winter from 15 individuals of *R. ferrumequinum* and 10 individuals of *M. petax* in the Jilin, Liaoning, Beijing and Henan provinces of China. A total of 15 bacterial samples from *R. ferrumequinum* were collected in Jilin (Da-lazi Cave:

2, Di Cave: 2, Xin Cave: 2, Ge-zi Cave: 5), Liaoning (Temple Cave: 2), Beijing (Bat Cave: 1) and Henan (Reservoir: 1). A total of 10 bacterial samples from *M. petax* were collected in Jilin (Xin Cave: 4, Ge-zi Cave: 4), and Liaoning (Temple Cave: 2). We wiped each bat's wing membrane with sterile cotton swabs dipped in sterile water. Swabs were then stored in 20% sterile glycerol at −80°C. These swabs were thawed and streaked across Reasoner's 2A agar (R2A) plates, which were incubated at 13°C for 2–5 days. According to the bacteria colony colour and morphology, different colonies were picked and streaked on a new R2A plate, and repeated twice until a purified strain was obtained. Each isolate was cryopreserved in 30% glycerol at −80°C for later use. The field work was approved by the Laboratory Animal Welfare and Ethics Committee of Jilin Agricultural University.

Agar plate challenge assays

Agar plate challenge assays were done on SDA according to the National Committee for Clinical Laboratory Standards. Three weeks–old *P. destructans* grown on SDA was soaked in 5 ml of 1X phosphate buffered saline with tween$_{20}$ (PBST$_{20}$) for 5 min, and then gently scraped to collect a conidial suspension. A total of 100 μl 2×10^5 *P. destructans* conidia ml^{-1} (counted using a haemocytometer) was then inoculated on SDA agar plates (90 mm × 18 mm) and dried for 20 min. After inoculation, bacterial isolate was placed at three evenly spaced points on top of the dried *P. destructans* suspension. Plates were incubated at 13°C and monitored every day until at 14 days, we observed a clear zone of inhibition around each bacterial colony. Control plates were made by spreading *P. destructans* suspension without bacterial isolate. All assays were conducted in triplicate.

Cell-free supernatant challenge assays

A cell-free supernatant assay was done in 96-well microplates based on previous work (Bell *et al.*, 2013). Bacterial isolates were inoculated in 10 ml of sterile Luria Broth (LB) liquid medium and cultured at 13°C for 60 h on a rotary shaker at 200 rpm. Isolates were then centrifuged at 8000 rpm for 10 min to obtain cell supernatants. We acquired *P. destructans* conidia by scraping plates with 1% tryptone broth. The experiment wells added 50 μl of 2×10^6 *P. destructans* conidia ml^{-1} and 50 μl of a bacterial cell-free supernatant sample. The positive control wells added 50 μl of *P. destructans* conidia and 50 μl of 1% tryptone broth. The negative control wells added 50 μl of heat-killed *P. destructans* (60°C for 45–60 min) conidia and 50 μl of 1% tryptone broth. Each experimental well and control well had twelve replicates. The microplates were incubated at 13°C, and absorbance values were recorded using a spectrophotometer at 492 nm from days 0 to 7 (maximum *P. destructans* growth). Inhibition score was calculated as follows: 1-[(-experiment$_{OD}$ − negative$_{OD}$)/(positive$_{OD}$ -negative$_{OD}$)] ×100. Analysis of variance (ANOVA) was used to identify the difference in inhibition between isolates. All analyses were performed in R v.3.6.0 (R Core Team, 2019).

Identification of bacterial isolates

We used PCR amplification and DNA sequencing technology to identify bacterial isolates that inhibited the growth of *P. destructans*. A single bacteria colony was picked with sterile toothpicks and dissolved in 100 μl of sterile deionized water (SDW), then boiled at 100°C for 10 min with using as a DNA template for PCR amplification. The common bacterial 16S rRNA gene primers 27F and 1429R were used in amplification (Fang *et al.*, 2016). The housekeeping *gyrB* gene (primers UP1E and APrU) was also used (Cladera *et al.*, 2004). The housekeeping *rpoD* gene (primers 70F and 70R) was PCR amplified as previously described (Yamamoto *et al.*, 2000). Similarly, the housekeeping *rpoB* gene (primers LAPS and LAPS27) was amplified as previously described (Ait Tayeb *et al.*, 2005). Our PCR system and conditions were as described previously (Mulet *et al.*, 2009). PCR products were forward and reverse sequenced, and spliced to obtain sequences using DNAStar 7.1 software, followed by manual inspection, and comparison with utilizing the GenBank database to identify the most similar sequence alignment.

Observation of the mycelial morphological changes of P. destructans *by treating with* P. yamanorum *GZD14026*

A small piece of *P. destructans* mycelium was cut from the inhibition zones on agar plates under the action of *P. yamanorum* GZD14026 at 14 days to make electron microscope samples. Non-treated mycelium was used as control. The samples were fixed in 3% glutaraldehyde for 24 h at room temperature and were then washed with deionized water for 30 min. Next, the samples were dehydrated for 30 min with 30%, 50%, 70%, 90% and 100% ethyl alcohol. Subsequently, samples were dried for 24 h at room temperature. The prepared samples were coated with gold particles and observed with a scanning electron microscope (SEM, FEI XL-30 ESEM-FEG, United States).

*Identification of anti-*P. destructans *active compounds*

Pseudomonas yamanorum GZD 14026 was grown in LB liquid medium for 3 days at 13°C on a rotary shaker

at 200 rpm. The liquid culture was centrifuged at 10 000 rpm for 10 min, and the cell-free culture supernatant was collected, followed by extraction with an equal volume of dichloromethane. The dichloromethane extracts were condensed in vacuo at 45°C to obtain crude extract. The crude extract was mixed with silica gel, and mixtures were eluted with a gradient from 100% dichloromethane to 100% methanol as a solvent system. The eluate was collected in bottles and detected by thin-layer chromatography (TLC). The fractions with similar results on TLC plates were then combined. These combined fractions were tested for anti-*P. destructans* activity with cell-free supernatant challenge assays. The active fraction then was crystallized under reduced pressure.

The active fraction was analysed by semi-preparative high-performance liquid chromatography (HPLC, Shimadzu LC8A, Japan). The mobile phase consisted of acetonitrile and 0.2% ice acetic acid, with a linear gradient from 10% to 100%, on a C18 reverse-phase column (Agilent ZORBAX SB-C18, 5 μm, 4.6 mm × 250 mm, United States) at a flow rate of 1.0 ml min^{-1} and detected at a wavelength of 250 nm. Meanwhile, the active fraction was measured by ultraviolet-visible spectroscopy (UV/Vis, Perkin Elmer Lambda 900, United States), mass spectrometry (MS, Waters ZQ2000, United States), and nuclear magnetic resonance (^{1}H NMR and ^{13}C NMR, BRUKER AVANCE III HD 500, Germany) were used to detect the pure active compound that was dissolved in deuteriated chloroform ($CDCl_3$) at room temperature.

*Evaluation of purified phenazine-1-carboxylic acid (PCA) for anti-*P. destructans *activity in vitro*

Based on our cell-free supernatant challenge assays, the minimal inhibitory concentration (MIC) and the half maximal inhibitory concentration (IC_{50}) of PCA to *P. destructans* were determined. Briefly, different concentrations of PCA and 2 × 10^5 *P. destructans* conidia suspension were transferred to a 96-well microplate for each reaction. DMSO (1%, v v^{-1}) was used as a solvent to dissolve PCA and as a negative control. Each microplate was incubated at 13°C for 7 days, and the absorbance at 492 nm was then recorded. All assays were conducted in triplicate.

DNA extraction and whole genome sequencing

Pseudomonas yamanorum GZD 14026 was grown in LB liquid medium for 3 days at 13°C on a rotary shaker at 200 rpm. The genomic DNA of strain GZD 14026 was extracted using the sodium dodecyl sulphate (SDS) method (Lim *et al*., 2016). The whole genome of *P. yamanorum* GZD 14026 was sequenced using the Pacific Biosciences (PacBio) Sequel platform.

Gene assembly and functional annotation

Filtered genome data were de novo assembled using the Single Molecule Real Time (SMRT) Link v. 5.0.1 program (Ardui *et al*., 2018). Six databases were used for gene functional annotation, including the Non-Redundant Protein (Li *et al*., 2002), Pfam, SwissProt (Bairoch and Apweiler, 2000; Finn *et al*., 2014), Gene Ontology and the Cluster of Orthologous Groups of proteins (Ashburner *et al*., 2000; Tatusov *et al*., 2003), the Kyoto Encyclopedia of Genes and Genomes databases (Kanehisa *et al*., 2004). Simultaneously, we utilized antiSMASH 4.0 (Blin *et al*., 2017) to analyse secondary metabolic gene clusters to verify the presence of active substance. The whole genome sequence of *P. yamanorum* GZD 14026 was submitted to the GenBank database with the accession number CP058644.

Co-culture assays P. yamanorum *GZD14026 with* P. destructans

A single-compartment Petri plate (200 mm × 30 mm) was used as a shared-airspace to assess *P. yamanorum* GZD14026 inhibition of the growth of *P. destructans* via volatile organic compounds. A total of 100 μl 2 × 10^5 *P. destructans* conidia ml^{-1} was spread on an SDA agar plate (90 mm × 18 mm). A 20 μl *P. yamanorum* GZD14026 suspension (suspended in LB liquid medium) was inoculated on an LB agar plate (90 mm × 18 mm) and cultured in this shared-airspace for up to 14 days at 13°C. All assays were conducted in triplicate.

*Evaluation the ability of volatile organic compounds anti-*P. destructans *from* P. yamanorum *GZD14026*

Volatile organic compounds from *P. yamanorum* GZD 14026 were collected using the headspace solid-phase micro-extraction (HS-SPME) technique that resulted in a shared-airspace inhibition of the growth of *P. destructans* after 14 days. *P. yamanorum* GZD 14026 was inoculated on LB agar (90 mm × 18 mm) for 14 days at 13°C. The blank control was an LB agar plate. All assays were conducted in triplicate. The headspace jars were added to cultured *P. yamanorum* GZD 14026 medium and heated at 40°C for 30 min. A SPME syringe containing 50/30 divinylbenzene/carburen in polydimethylsiloxane on a stable fibre (65 μm) was inserted into these headspace jars and exposed for 20 min. Then, the syringe was pulled out from the headspace jar and inserted into a gas chromatography-mass spectrometry (GC-MS, Agilent 5975, United States). A capillary

column (30 m × 0.25 mm × 0.25 μm, Agilent DB-5MS, United States) was used to spread these volatile organic compounds. The oven temperature was 40°C and was held for 3 min, ramped at 5°C min^{-1} to 180°C and then ramped at 20°C min^{-1} to 230°C, where the temperature was then held for 5 min. The temperatures of the transfer line and ion trap were 250°C and 200°C, respectively. Identification of volatile organic compounds was based on the National Institute of Standards and Technology (NIST) spectra database.

To test the inhibition *P. destructans* effect of volatile organic compounds, sterile filter paper containing 10 or 100 ppm (μg ml^{-1}) octanoic acid, 3-methyl-3-buten-1-ol or 3-tert-butyl-4-hydroxyanisole was placed on one side of a Petri plate (90 mm × 18 mm), while the other side was inoculated with 100 μl of 2 × 10^5 *P. destructans* on SDA. The 3-tert-butyl-4-hydroxyanisole was diluted in 95% ethanol. Dilute sterile filter paper with 95% ethanol was used as a control. Plates were incubated at 13°C and monitored every day until 14 days observing the growth of *P. destructans*. The identified volatile organic compounds were purchased from Sigma-Aldrich and Aladdin.

Acknowledgements

We are grateful to Zhongwei Yin for his help in sampling in the field, and Wenlong Dong for his assistance in my laboratory work.

Conflict of interest

The authors declare no conflict of interests.

Author contributions

ZL performed laboratory work and data analysis, and drafted the manuscript. ZL, AL, WD, JRH, HL, LJ and SL collected the samples. YL and WL guided the laboratory work. KS and JF developed the study concept, design, and supervised the project. KS and JRH reviewed and revised the manuscript.

References

Ait Tayeb, L., Ageron, E., Grimont, F., and Grimont, P.A. (2005) Molecular phylogeny of the genus *Pseudomonas* based on *rpoB* sequences and application for the identification of isolates. *Res Microbiol* **156:** 763–773.

Annamalai, T., Nair, M.K.M., Marek, P., Vasudevan, P., Schreiber, D., Knight, R., *et al*. (2004) In vitro inactivation of *Escherichia coli* O157: H7 in bovine rumen fluid by caprylic acid. *J Food Protect* **67:** 884–888.

Ardui, S., Ameur, A., Vermeesch, J.R., and Hestand, M.S. (2018) Single molecule real-time (SMRT) sequencing comes of age: applications and utilities for medical diagnostics. *Nucleic Acids Res* **46:** 2159–2168.

Arnau, V.G., Sánchez, L.A., and Delgado, O.D. (2015) *Pseudomonas yamanorum* sp. nov., a psychrotolerant bacterium isolated from a subantarctic environment. *Int J Syst Evol Micr* **65:** 424–431.

Ashburner, M., Ball, C.A., Blake, J.A., Botstein, D., Butler, H., Cherry, J.M., *et al*. (2000) The Gene Ontology Consortium. *Nat Genet* **25:** 25–29.

Bahroun, A., Jousset, A., Mhamdi, R., Mrabet, M., and Mhadhbi, H. (2018) Anti-fungal activity of bacterial endophytes associated with legumes against *Fusarium solani*: Assessment of fungi soil suppressiveness and plant protection induction. *Appl Soil Ecol* **124:** 131–140.

Bairoch, A., and Apweiler, R. (2000) The SWISS-PROT protein sequence database and its supplement TrEMBL in 2000. *Nucleic Acids Res* **28:** 45–48.

Bell, S.C., Alford, R.A., Garland, S., Padilla, G., and Thomas, A.D. (2013) Screening bacterial metabolites for inhibitory effects against *Batrachochytrium dendrobatidis* using a spectrophotometric assay. *Dis Aquat Organ* **103:** 77–85.

Bender, C., Rangaswamy, V., and Loper, J. (1999) Polyketide production by plant-associated pseudomonads. *Annu Rev Phytopathol* **37:** 175–196.

Blin, K., Wolf, T., Chevrette, M.G., Lu, X., Schwalen, C.J., Kautsar, S.A., *et al*. (2017) antiSMASH 4.0-improvements in chemistry prediction and gene cluster boundary identification. *Nucleic Acids Res* **45:** W36–41.

Brockmann, M., Aupperle-Lellbach, H., Gentil, M., Heusinger, A., Müller, E., Marschang, R.E., and Pees, M. (2020) Challenges in microbiological identification of aerobic bacteria isolated from the skin of reptiles. *PLoS One* **15:** e0240085.

Brunetti, A.E., Lyra, M.L., Melo, W.G.P., Andrade, L.E., Palacios-Rodríguez, P., Prado, B.M., *et al*. (2019) Symbiotic skin bacteria as a source for sex-specific scents in frogs. *Proc Natl Acad Sci USA* **116:** 2124–2129.

Cecotti, R., Carpana, E., Falchero, L., Paoletti, R., and Tava, A. (2012) Determination of the volatile fraction of *Polygonum bistorta* L. at different growing stages and evaluation of its antimicrobial activity against two major honeybee (*Apis mellifera*) pathogens. *Chem Biodivers* **9:** 359–369.

Chang, H.T., and Branen, A. (1975) Antimicrobial effects of butylated hydroxyanisole (BHA). *J Food Sci* **40:** 349–351.

Cladera, A.M., Bennasar, A., Barceló, M., Lalucat, J., and García-Valdés, E. (2004) Comparative genetic diversity of *Pseudomonas stutzeri* genomovars, clonal structure, and phylogeny of the species. *J Bacteriol* **186:** 5239–5248.

Cornelison, C.T., Keel, M.K., Gabriel, K.T., Barlament, C.K., Tucker, T.A., Pierce, G.E., and Crow, S.A. (2014) A preliminary report on the contact-independent antagonism of *Pseudogymnoascus destructans* by *Rhodococcus rhodochrous* strain DAP96253. *BMC Microbiol* **14:** 246.

Elkahoui, S., Djébali, N., Yaich, N., Azaiez, S., Hammami, M., Essid, R., and Limam, F. (2015) Antifungal activity of volatile compounds-producing *Pseudomonas* P2 strain against *Rhizoctonia solani*. *World J Microbiol Biotechnol* **31:** 175–185.

Fang, Z., Yao, W., Lou, X., Hao, C., Gong, C., and Ouyang, Z. (2016) Profile and characteristics of culturable airborne

bacteria in Hangzhou, southeast of China. *Aerosol Air Qual Res* **16:** 1690–1700.

Fernandez, M., Godino, A., Príncipe, A., López Ramírez, V., Quesada, J.M., Rigo, V., *et al*. (2020) Characterization of the bacteriocins and the PrtR regulator in a plant-associated *Pseudomonas* strain. *J Biotechnol* **307:** 182–192.

Finn, R.D., Bateman, A., Clements, J., Coggill, P., Eberhardt, R.Y., Eddy, S.R., *et al*. (2014) Pfam: the protein families database. *Nucleic Acids Res* **42:** D222–230.

Frick, W.F., Pollock, J.F., Hicks, A.C., Langwig, K.E., Reynolds, D.S., Turner, G.G., *et al*. (2010) An emerging disease causes regional population collapse of a common North American bat species. *Science* **329:** 679–682.

Gargas, A., Trest, M., Christensen, M., Volk, T.J., and Blehert, D.S. (2009) *Geomyces destructans* sp. nov., associated with bat white-nose syndrome. *Mycotaxon* **108:** 147–154.

George, K.W., Thompson, M.G., Kang, A., Baidoo, E., Wang, G., Chan, L.J., *et al*. (2015) Metabolic engineering for the high-yield production of isoprenoid-based C_5 alcohols in *E. coli*. *Sci Rep* **5:** 11128.

Gholami, S., Tabatabaei, M., and Sohrabi, N. (2017) Comparison of biofilm formation and antibiotic resistance pattern of *Pseudomonas aeruginosa* in human and environmental isolates. *Microb Pathog* **109:** 94–98.

Haas, D., Blumer, C., and Keel, C. (2000) Biocontrol ability of fluorescent pseudomonads genetically dissected: importance of positive feedback regulation. *Curr Opin Biotech* **11:** 290–297.

Hamm, P.S., Caimi, N.A., Northup, D.E., Valdez, E.W., Buecher, D.C., Dunlap, C.A., *et al*. (2017) Western bats as a reservoir of novel *Streptomyces* species with antifungal activity. *Appl Environ Microbiol* **83:** e03057-16.

Hoyt, J.R., Cheng, T.L., Langwig, K.E., Hee, M.M., Frick, W.F., and Kilpatrick, A.M. (2015) Bacteria isolated from bats inhibit the growth of *Pseudogymnoascus destructans*, the causative agent of white-nose syndrome. *PLoS One* **10:** e0121329.

Hoyt, J.R., Langwig, K.E., Sun, K., Lu, G., Parise, K.L., Jiang, T., *et al*. (2016a) Host persistence or extinction from emerging infectious disease: insights from white-nose syndrome in endemic and invading regions. *Proc Roy Soc B-Biol Sci* **283:** 20152861.

Hoyt, J.R., Langwig, K.E., White, J.P., Kaarakka, H.M., Redell, J.A., Parise, K.L., *et al*. (2019) Field trial of a probiotic bacteria to protect bats from white-nose syndrome. *Sci Rep* **9:** 1–9.

Hoyt, J.R., Langwig, K.E., Sun, K., Parise, K.L., Li, A., Wang, Y., *et al*. (2020) Environmental reservoir dynamics predict global infection patterns and population impacts for the fungal disease white-nose syndrome. *Proc Natl Acad Sci USA* **117:** 7255–7262.

Hoyt, J.R., Sun, K., Parise, K.L., Lu, G., Langwig, K.E., Jiang, T., *et al*. (2016b) Widespread bat white-nose syndrome fungus, northeastern China. *Emerg Infect Dis* **22:** 140.

Huasong, P., Qingwen, H., Bilal, M., Wang, W., and Zhang, X. (2020) Kinetics, mechanism, and identification of photodegradation products of phenazine-1-carboxylic acid. *Environ Technol* **41:** 1848–1856.

Isnansetyo, A., Cui, L., Hiramatsu, K., and Kamei, Y. (2003) Antibacterial activity of 2, 4-diacetylphloroglucinol produced by *Pseudomonas* sp. AMSN isolated from a marine alga, against vancomycin-resistant *Staphylococcus aureus*. *Int J Antimicrob Ag* **22:** 545–547.

Jeon, B.S., Kim, S., and Sang, B.I. (2017) *Megasphaera hexanoica* sp. nov., a medium-chain carboxylic acid-producing bacterium isolated from a cow rumen. *Int J Syst Evol Microbiol* **67:** 2114–2120.

Jin, Z.J., Zhou, L., Sun, S., Cui, Y., Song, K., Zhang, X., and He, Y.W. (2020) Identification of a strong quorum sensing- and thermo-regulated promoter for the biosynthesis of a new metabolite pesticide phenazine-1-carboxamide in *Pseudomonas* strain PA1201. *ACS Synth Biol* **9:** 1802–1812.

Kamou, N.N., Cazorla, F., Kandylas, G., and Lagopodi, A.L. (2020) Induction of defense-related genes in tomato plants after treatments with the biocontrol agents *Pseudomonas chlororaphis* ToZa7 and *Clonostachys rosea* IK726. *Arch Microbiol* **202:** 257–267.

Kanehisa, M., Goto, S., Kawashima, S., Okuno, Y., and Hattori, M. (2004) The KEGG resource for deciphering the genome. *Nucleic Acids Res* **32:** D277–D280.

Kerry, R.G., Patra, J.K., Gouda, S., Park, Y., Shin, H.-S., and Das, G. (2018) Benefaction of probiotics for human health: a review. *J Food Drug Anal* **26:** 927–939.

Kim, K.J. (2000) Phenazine 1-carboxylic acid resistance in phenazine 1-carboxylic acid producing *Bacillus* sp. B-6. *BMB Reports* **33:** 332–336.

Kollanoor, A., Vasudevan, P., Nair, M.K.M., Hoagland, T., and Venkitanarayanan, K. (2007) Inactivation of bacterial fish pathogens by medium-chain lipid molecules (caprylic acid, monocaprylin and sodium caprylate). *Aquac Res* **38:** 1293–1300.

Kruger, A. (2020) Functional redundancy of *Batrachochytrium dendrobatidis* inhibition in bacterial communities isolated from *Lithobates clamitans* skin. *Microb Ecol* **79:** 231–240.

Langwig, K.E., Frick, W.F., Bried, J.T., Hicks, A.C., Kunz, T.H., and Kilpatrick, A.M. (2012) Sociality, density-dependence and microclimates determine the persistence of populations suffering from a novel fungal disease, white-nose syndrome. *Ecol Lett* **15:** 1050–1057.

Laursen, J.B., and Nielsen, J. (2004) Phenazine natural products: biosynthesis, synthetic analogues, and biological activity. *Chem Rev* **104:** 1663–1686.

Lee, J.Y., Moon, S.S., and Hwang, B.K. (2003) Isolation and *in vitro* and *in vivo* activity against *Phytophthora capsici* and *Colletotrichum orbiculare* of phenazine-1-carboxylic acid from *Pseudomonas aeruginosa* strain GC - B26. *Pest Manag Sci* **59:** 872–882.

Li, W., Jaroszewski, L., and Godzik, A. (2002) Tolerating some redundancy significantly speeds up clustering of large protein databases. *Bioinformatics* **18:** 77–82.

Lim, H.J., Lee, E.H., Yoon, Y., Chua, B., and Son, A. (2016) Portable lysis apparatus for rapid single-step DNA extraction of *Bacillus subtilis*. *J Appl Microbiol* **120:** 379–387.

Lorch, J.M., Knowles, S., Lankton, J.S., Michell, K., Edwards, J.L., Kapfer, J.M., *et al*. (2016) Snake fungal disease: an emerging threat to wild snakes. *Philos Trans R Soc Lond B Biol Sci* **371.**

Lorch, J.M., Meteyer, C.U., Behr, M.J., Boyles, J.G., Cryan, P.M., Hicks, A.C., *et al*. (2011) Experimental infection of

bats with *Geomyces destructans* causes white-nose syndrome. *Nature* **480:** 376–378.

Markowiak, P., Śliżewska, K., Nowak, A., Chlebicz, A., Żbikowski, A., Pawłowski, K., and Szeleszczuk, P. (2019) Probiotic microorganisms detoxify ochratoxin A in both a chicken liver cell line and chickens. *J Sci Food Agric* **99:** 4309–4318.

Mavrodi, D.V., Blankenfeldt, W., and Thomashow, L.S. (2006) Phenazine compounds in fluorescent *Pseudomonas* spp. biosynthesis and regulation. *Annu Rev Phytopathol* **44:** 417–445.

Mavrodi, D.V., Ksenzenko, V.N., Bonsall, R.F., Cook, R.J., Boronin, A.M., and Thomashow, L.S. (1998) A seven-gene locus for synthesis of phenazine-1-carboxylic acid by *Pseudomonas fluorescens* 2–79. *J Bacteriol* **180:** 2541–2548.

McArthur, R.L., Ghosh, S., and Cheeptham, N. (2017) Improvement of protocols for the screening of biological control agents against white-nose syndrome. *JEMI* **2:** 1–7.

Micalizzi, E.W., Mack, J.N., White, G.P., Avis, T.J., and Smith, M.L. (2017) Microbial inhibitors of the fungus *Pseudogymnoascus destructans*, the causal agent of white-nose syndrome in bats. *PLoS One* **12:** e0179770.

Micalizzi, E.W., and Smith, M.L. (2020) Volatile organic compounds kill the white-nose syndrome fungus, *Pseudogymnoascus destructans*, in hibernaculum sediment. *Can J Microbiol* **66:** 593–599.

Mossine, V.V., Chance, D.L., Waters, J.K., and Mawhinney, T.P. (2018) Interaction of bacterial phenazines with colistimethate in bronchial epithelial cells. *Antimicrob Agents Chemother* **62:** e02349-17.

Mulet, M., Bennasar, A., Lalucat, J., and García-Valdés, E. (2009) An *rpoD*-based PCR procedure for the identification of *Pseudomonas* species and for their detection in environmental samples. *Mol Cell Probes* **23:** 140–147.

Nair, M.K.M., Vasudevan, P., Hoagland, T., and Venkitanarayanan, K. (2004) Inactivation of *Escherichia coli* O157: H7 and *Listeria monocytogenes* in milk by caprylic acid and monocaprylin. *Food Microbiol* **21:** 611–616.

Nielsen, T., Sørensen, D., Tobiasen, C., Andersen, J.B., Christophersen, C., Givskov, M., and Sørensen, J. (2002) Antibiotic and biosurfactant properties of cyclic lipopeptides produced by fluorescent *Pseudomonas* spp. from the sugar beet rhizosphere. *Appl Environ Microb* **68:** 3416–3423.

Olasehinde, T.A., Olaniran, A.O., and Okoh, A.I. (2020) Cholinesterase inhibitory activity, antioxidant properties, and phytochemical composition of *Chlorococcum* sp. extracts. *J Food Biochem* **27:** e13395.

Pierson, M.D., Smoot, L.A., and Vantassell, K.R. (1980) Inhibition of *Salmonella typhimurium* and *Staphylococcus aureus* by Butylated Hydroxyanisole and the Propyl Ester of p-Hydroxybenzoic Acid. *J Food Prot* **43:** 191–194.

R Core Team (2019) *R: A Language and Environment for Statistical Computing*. Vienna, Austria: R Foundation for Statistical Computing.

Rajkumar, K., Mvs, S., Koganti, S., and Burgula, S. (2020) Selenium nanoparticles synthesized Using *Pseudomonas stutzeri* (MH191156) show antiproliferative and anti-angiogenic activity against cervical cancer cells. *Int J Nanomedicine* **15:** 4523–4540.

Raudabaugh, D.B., and Miller, A.N. (2015) Effect of trans, trans-farnesol on *Pseudogymnoascus destructans* and several closely related species. *Mycopathologia* **180:** 325–332.

Rusman, Y., Wilson, M.B., Williams, J.M., Held, B.W., Blanchette, R.A., Anderson, B.N., *et al*. (2020) Antifungal norditerpene oidiolactones from the fungus *Oidiodendron truncatum*, a potential biocontrol agent for white-nose syndrome in bats. *J Nat Prod* **83:** 344–353.

Santos Kron, A., Zengerer, V., Bieri, M., Dreyfuss, V., Sostizzo, T., Schmid, M., *et al*. (2020) *Pseudomonas orientalis* F9 pyoverdine, safracin, and phenazine mutants remain effective antagonists against *Erwinia amylovora* in apple flowers. *Appl Environ Microbiol* **86:** e02620-19.

Sasaki, Y., Eng, T., Herbert, R.A., Trinh, J., Chen, Y., Rodriguez, A., *et al*. (2019) Engineering *Corynebacterium glutamicum* to produce the biogasoline isopentenol from plant biomass hydrolysates. *Biotechnol Biofuels* **12:** 41.

Scheele, B., Pasmans, F., Skerratt, L.F., Berger, L., Martel, A., Beukema, W., *et al*. (2019) Amphibian fungal panzootic causes catastrophic and ongoing loss of biodiversity. *Science* **363:** 1459–1463.

Schnider, U., Keel, C., Blumer, C., Troxler, J., Défago, G., and Haas, D. (1995) Amplification of the housekeeping sigma factor in *Pseudomonas fluorescens* CHA0 enhances antibiotic production and improves biocontrol abilities. *J Bacteriol* **177:** 5387–5392.

Shen, X., Chen, M., Hu, H., Wang, W., Peng, H., Xu, P., and Zhang, X. (2012) Genome sequence of *Pseudomonas chlororaphis* GP72, a root-colonizing biocontrol strain. *J Bacteriol* **194:** 1269–1270.

Skerratt, L.F., Berger, L., Speare, R., Cashins, S., McDonald, K.R., Phillott, A.D., *et al*. (2007) Spread of chytridiomycosis has caused the rapid global decline and extinction of frogs. *EcoHealth* **4:** 125–134.

Tan, L.-T.-H., Chan, K.-G., Lee, L.-H., and Goh, B.-H. (2016) *Streptomyces* bacteria as potential probiotics in aquaculture. *Front Microbiol* **7:** 79.

Tatusov, R.L., Fedorova, N.D., Jackson, J.D., Jacobs, A.R., Kiryutin, B., Koonin, E.V., *et al*. (2003) The COG database: an updated version includes eukaryotes. *BMC Bioinformatics* **4:** 41.

Vignatti, P., Gonzalez, M.E., Jofré, E.C., Bolívar-Anillo, H.J., Moraga, J., Viaud, M., *et al*. (2020) Botrydial confers *Botrytis cinerea* the ability to antagonize soil and phyllospheric bacteria. *Fungal Biol* **124:** 54–64.

Wang, Z., Mei, X., Du, M., Chen, K., Jiang, M., Wang, K., *et al*. (2020) Potential modes of action of *Pseudomonas fluorescens* ZX during biocontrol of blue mold decay on postharvest citrus. *J Sci Food Agric* **100:** 744–754.

Warnecke, L., Turner, J.M., Bollinger, T.K., Lorch, J.M., Misra, V., Cryan, P.M., *et al*. (2012) Inoculation of bats with European *Geomyces destructans* supports the novel pathogen hypothesis for the origin of white-nose syndrome. *Proc Natl Acad Sci USA* **109:** 6999–7003.

Wibbelt, G., Kurth, A., Hellmann, D., Weishaar, M., Barlow, A., Veith, M., *et al*. (2010) White-nose syndrome fungus (*Geomyces destructans*) in bats, Europe. *Emerg Infect Dis* **16:** 1237–1243.

Xia, B., Yu, J., He, T., Liu, X., Su, J., Wang, M., *et al.* (2020) *Lactobacillus johnsonii* L531 ameliorates enteritis via elimination of damaged mitochondria and suppression of SQSTM1- dependent mitophagy in a *Salmonella* infantis model of piglet diarrhea. *FASEB J* **34:** 2821–2839.

Xiong, Z., Niu, J., Liu, H., Xu, Z., Li, J., and Wu, Q. (2017) Synthesis and bioactivities of Phenazine-1-carboxylic acid derivatives based on the modification of PCA carboxyl group. *Bioorg Med Chem Lett* **27:** 2010–2013.

Xu, S., Pan, X., Luo, J., Wu, J., Zhou, Z., Liang, X., *et al.* (2015) Effects of phenazine-1-carboxylic acid on the biology of the plant-pathogenic bacterium *Xanthomonas oryzae* pv. *oryzae*. *Pestic Biochem Physiol* **117:** 39–46.

Yamamoto, S., Kasai, H., Arnold, D.L., Jackson, R.W., Vivian, A., and Harayama, S. (2000) Phylogeny of the genus *Pseudomonas*: intrageneric structure reconstructed from the nucleotide sequences of *gyrB* and *rpoD* genes. *Microbiology* **146:** 2385–2394.

Yuan, L.L., Li, Y.Q., Wang, Y., Zhang, X.H., and Xu, Y.Q. (2008) Optimization of critical medium components using response surface methodology for phenazine-1-carboxylic acid production by *Pseudomonas* sp. M-18Q. *J Biosci Bioeng* **105:** 232–237.

Zhang, L., Tian, X., Kuang, S., Liu, G., Zhang, C., and Sun, C. (2017) Antagonistic activity and mode of action of phenazine-1-carboxylic acid, produced by marine bacterium *Pseudomonas aeruginosa* PA31x, against *Vibrio anguillarum in vitro* and in a zebrafish *in vivo* model. *Front Microbiol* **8:** 289.

Zhou, Q., Su, J., Jiang, H., Huang, X., and Xu, Y. (2010) Optimization of phenazine-1-carboxylic acid production by a *gacA/qscR*-inactivated *Pseudomonas* sp. M18GQ harboring pME6032Phz using response surface methodology. *Appl Microbiol Biot* **86:** 1761–1773.

Zhu, X., Zeng, Y., Zhao, X., Zou, S., He, Y.W., and Liang, Y. (2017) A genetic screen in combination with biochemical analysis in *Saccharomyces cerevisiae* indicates that phenazine-1-carboxylic acid is harmful to vesicular trafficking and autophagy. *Sci Rep* **7:** 1967.

Supporting information

Additional supporting information may be found online in the Supporting Information section at the end of the article.

Fig. S1. Identification of the structure of the active compound working against *P. destructans* from *P. yamanorum* GZD 14026. A. UV/Vis detection of the active compound. Absorbance × Wavelength. B. (a) ^{1}H spectral and ^{13}C spectral (b) of the active compound. C. The chemical structure of phenazine-1-carboxylic acid (PCA).

Table S1. Volatile organic compounds produced by *P. yamanomum* GZD 14026 after 14 days.

